⌘ *Author's Choice*

THE JOURNAL OF BIOLOGICAL CHEMISTRY VOL. 285, NO. 18, pp. 13542–13549, April 30, 2010

Identification of Functionally Segregated Sarcoplasmic Reticulum Calcium Stores in Pulmonary Arterial Smooth Muscle*

Received for publication, January 6, 2010, and in revised form, February 11, 2010 Published, JBC Papers in Press, February 21, 2010, DOI 10.1074/jbc.M110.101485

Jill H. Clark[‡], Nicholas P. Kinnear[‡], Svetlana Kalujnaia[§], Gordon Cramb[§], Sidney Fleischer[¶‖], Loice H. Jeyakumar[**], Frank Wuytack[‡‡], and A. Mark Evans[‡1]

*From the [‡]Centre for Integrative Physiology, College of Medicine and Veterinary Medicine, University of Edinburgh, Edinburgh EH8 9XD, United Kingdom, the [§]School of Medicine, University of St. Andrews, St. Andrews, United Kingdom, the [¶]Department of Biological Sciences, Vanderbilt University, Nashville, Tennessee 37232, the [‖]Department of Pharmacology and **Department of Medicine/Gastroenterology, Vanderbilt University Medical School, Nashville, Tennessee 37235, and [‡‡]Laboratory of Ca^{2+}-Transport ATPases, Department of Molecular Cell Biology, Katholieke Universiteit Leuven, B-3000 Leuven, Belgium*

In pulmonary arterial smooth muscle, Ca^{2+} release from the sarcoplasmic reticulum (SR) via ryanodine receptors (RyRs) may induce constriction and dilation in a manner that is not mutually exclusive. We show here that the targeting of different sarcoplasmic/endoplasmic reticulum Ca^{2+}-ATPases (SERCA) and RyR subtypes to discrete SR regions explains this paradox. Western blots identified protein bands for SERCA2a and SERCA2b, whereas immunofluorescence labeling of isolated pulmonary arterial smooth muscle cells revealed striking differences in the spatial distribution of SERCA2a and SERCA2b and RyR1, RyR2, and RyR3, respectively. Almost all SERCA2a and RyR3 labeling was restricted to a region within 1.5 μm of the nucleus. In marked contrast, SERCA2b labeling was primarily found within 1.5 μm of the plasma membrane, where labeling for RyR1 was maximal. The majority of labeling for RyR2 lay in between these two regions of the cell. Application of the vasoconstrictor endothelin-1 induced global Ca^{2+} waves in pulmonary arterial smooth muscle cells, which were markedly attenuated upon depletion of SR Ca^{2+} stores by preincubation of cells with the SERCA inhibitor thapsigargin but remained unaffected after preincubation of cells with a second SERCA antagonist, cyclopiazonic acid. We conclude that functionally segregated SR Ca^{2+} stores exist within pulmonary arterial smooth muscle cells. One sits proximal to the plasma membrane, receives Ca^{2+} via SERCA2b, and likely releases Ca^{2+} via RyR1 to mediate vasodilation. The other is located centrally, receives Ca^{2+} via SERCA2a, and likely releases Ca^{2+} via RyR3 and RyR2 to initiate vasoconstriction.

Previous studies on smooth muscle have provided evidence in support of the view that the sarcoplasmic reticulum (SR)[2] may be functionally segregated (1, 2). Evidence suggests that such segregation may confer functionally segregated Ca^{2+} stores that may be mobilized differentially and in a stimulus-specific manner. Briefly, it has been shown that: 1) preincubation of pulmonary arterial smooth muscle with ryanodine, both with and without caffeine, may block Ca^{2+} signals via ryanodine receptor (RyR) activation without affecting Ca^{2+}signals generated in response to IP_3 (3, 4); 2) both caffeine-sensitive and caffeine-insensitive SR stores exist in cultured mesenteric arterial smooth muscle and airway smooth muscle cells, with only the latter sensitive to depletion by the sarco/endoplasmic reticulum Ca^{2+}-ATPase (SERCA) antagonist cyclopiazonic acid (5–7); and 3) activation of β-adrenoceptors on airway smooth muscle cells may increase the Ca^{2+} concentration in the subplasmalemmal region while decreasing the Ca^{2+} concentration in the central cytoplasmic region (8).

Our investigations on pulmonary arterial smooth muscle have provided further support for the view that functionally segregated SR stores may exist. We demonstrated that β-adrenoreceptor activation mobilizes Ca^{2+}, via RyRs, from a cyclopiazonic acid-sensitive SR store proximal to the plasma membrane and thereby recruits large conductance Ca^{2+}-activated K^+ (BK_{Ca}) channels, leading to smooth muscle cell hyperpolarization and pulmonary artery dilation (9). In itself this may not seem surprising, except for the fact that in these studies cyclopiazonic acid was without effect on artery constriction by prostaglandin $F_{2\alpha}$, which induces constriction in part by mobilizing ryanodine-sensitive SR stores (10, 11). Therefore, both preconstriction and subsequent vasodilation in response to β-adrenoreceptor activation were, at least in part, mediated by Ca^{2+} release from what is considered to be a continuous (*i.e.* the same) SR store (12). This paradox and the findings of others (see above) could be explained by the presence of two functionally and spatially segregated SR compartments, each equipped with a specific SERCA-type Ca^{2+} pump and a specific RyR-type Ca^{2+} release channel (for review see Ref. 13). This is quite possible given that all three RyR subtypes (14) are expressed in arterial smooth muscle (15–18), and a family of three genes encodes multiple SERCA pumps (19–22), namely the alterna-

* This work was funded by British Heart Foundation Project Grants PG/03/065 and PG/05/128 and by Grant G.0646.08 from the Fonds voor Wetenschappelijk Onderzoek Vlaanderen (to F. W.).

⌘ *Author's Choice*—Final version full access.

[1] To whom correspondence should be addressed: Centre for Integrative Physiology, College of Medicine and Veterinary Medicine, University of Edinburgh, Hugh Robson Bldg., George Square, Edinburgh EH8 9XD, UK. Fax: 44-131-650-6527; E-mail: mark.evans@ed.ac.uk.

[2] The abbreviations used are: SR, sarcoplasmic reticulum; SERCA, sarcoplasmic/endoplasmic reticulum Ca^{2+}-ATPase(s); RyR, ryanodine receptor; BK_{Ca}, large conductance Ca^{2+}-activated potassium channel; RT, reverse transcription; DAPI, 4′,6′-diamino-2-phenylindole; PASMC, pulmonary arterial smooth muscle cell; ET-1, endothelin-1.

TABLE 1
Primers for RT-PCR experiments GenBank™ accession numbers NM_058213 (SERCA1), J04023 (SERCA2a), J04022 (SERCA2b), and J05086 (SERCA3)

Gene	Primer	Sequence	Nucleotide positions	Predicted product size
				bp
SERCA1	Sense	CTC ACT TCC AGT CAT CGG GCT AG	3084–3106	340
	Antisense	GTC AGC TAG TTG CCT TGT CCC TG	3423–3401	
SERCA2a	Sense	CCT GTC CAG TTA CTC TGG GTC	2569–2589	694
	Antisense	GCT AAC AAC GCA CAT GCA CGC	3262–3242	
SERCA2b	Sense	GCC AAC ATT GCC TAT TCA GTG GCA C	4382–4406	501
	Antisense	GGA TGT TGG AAG GCA TTG GAG G	4882–4861	
SERCA3	Sense	CTC WGA GAA CCA GTC ACT GCT GC[a]	2879–2901	264
	Antisense	GCT CYC AGG ATT TAC TTC AGG TCC[b]	3142–3119	

[a] W indicates A or T.
[b] Y indicates C or T.

tively spliced isoforms SERCA1a and SERCA1b (23, 24), the SERCA2a and SERCA2b isoforms (23, 25–28), and SERCA3a–f (22, 29, 30). We therefore sought to determine whether or not multiple SERCA isoforms were expressed in pulmonary arterial smooth muscle cells and, if so, whether or not different SERCA and RyR subtypes were differentially distributed in pulmonary arterial smooth muscle cells in a manner consistent with the presence of two functionally segregated SR compartments.

EXPERIMENTAL PROCEDURES

All of the experiments were performed under the United Kingdom Animals (Scientific Procedures) Act of 1986. Adult male Wistar rats (150–300 g) were sacrificed by cervical dislocation. Skeletal muscle, brain, heart, and lungs were removed and placed on ice in physiological salt solution of the following composition: 130 mmol/liter NaCl, 5.2 mmol/liter KCl, 1 mmol/liter $MgCl_2$, 1.7 mmol/liter $CaCl_2$, 10 mmol/liter glucose, and 10 mmol/liter Hepes, pH 7.45.

RT-PCR—Total RNA was extracted from second and third order branches of the pulmonary arterial tree, heart, brain, and skeletal muscle using TRIzol® reagent according to the manufacturer's instructions (Invitrogen). Reverse transcription was carried out using 6 μg of RNA and 200 units of Moloney murine leukemia virus (Promega), and PCR was performed on 1 μl of cDNA with 1 unit/μl *Taq* DNA polymerase (Biogene) as previously described (31). The primers used for each receptor are shown in Table 1. All of the primer sequences were checked against the GenBank™, and no cross-reactivity was found. The RT-PCR products over 40 cycles of amplification were resolved by electrophoresis in 1% agarose gels and visualized under UV illumination using an image capture system (Genesnap image analysis system; Syngene).

Western Blotting—Second order branches of the pulmonary arterial tree, heart, brain, and skeletal muscle were rapidly frozen in liquid nitrogen. Small segments of tissue were ground to a powder under liquid nitrogen and homogenized in an appropriate volume of ice-cold buffer (50 mmol/liter Tris, 150 mmol/liter NaCl, 50 mmol/liter NaF, 5 mmol/liter sodium pyrophosphate, 1 mmol/liter EDTA, 1 mmol/liter EGTA, 1 mmol/liter dithiothreitol, 0.1 mmol/liter benzamidine, 0.1 mmol/liter phenylmethylsulfonyl fluoride, 0.2 mmol/liter mannitol, 0.1% (v/v) Triton, pH 7.4) using a motor-driven pestle. The homogenate was kept on ice for 30 min and then centrifuged (7500 rpm, 5 min, 4 °C). The supernatants were removed, and their protein concentrations were determined.

Equal amounts of homogenates (free of nuclear and whole cell debris) were separated on 10% bisacrylamide gels (NuPAGE™ electrophoresis system; Invitrogen) and blotted onto nitrocellulose membranes. The blots were probed with sequence-specific antibodies for SERCA1 (1:2500, mouse monoclonal, raised against residues 199–505 of rabbit SERCA1; Abcam), SERCA2a (1:10000, rabbit polyclonal, raised against residues 989–997 of pig SERCA2a; F. Wuytack, Leuven, Belgium (30, 32)), SERCA2b (1:5000, rabbit polyclonal, raised against residues 1032–1043 of pig SERCA2b; F. Wuytack, Leuven, Belgium (30, 32)), and SERCA3 (1:500, rabbit polyclonal, raised against residues 29–39 of mouse SERCA3; Abcam). Every blot was also probed with a polyclonal antibody for actin to ensure equal protein loading (Sigma) alongside the SERCA antibodies. Detection was performed with horseradish peroxide-conjugated secondary antibodies using the ECL system (GE Healthcare).

Smooth Muscle Cell Isolation—Single arterial smooth muscle cells were isolated from second order branches of the pulmonary artery. Briefly, the arteries were dissected out and placed in low Ca^{2+} solution of the following composition: 124 mM NaCl, 5 mM KCl, 1 mM $MgCl_2$, 0.5 mM NaH_2PO_4, 0.5 mM KH_2PO, 15 mM $NaHCO_3$, 0.16 mM $CaCl_2$, 0.5 mM EDTA, 10 mM glucose, 10 mM taurine, and 10 mM Hepes, pH 7.4. After 10 min the arteries were placed in the same solution containing 0.5 mg/ml papain and 1 mg/ml bovine serum albumin and kept at 4 °C overnight. The following day 0.2 mmol/liter 1,4-dithio-DL-threitol was added to the solution to activate the protease, and the preparation was incubated for 1 h at room temperature (22 °C). The tissue was then washed three times in fresh low Ca^{2+} solution without enzymes, and single smooth muscle cells were isolated by gentle trituration with a fire-polished Pasteur pipette. The cells were stored in suspension at 4 °C until required.

Immunocytochemistry—The cells were placed onto poly-D-lysine-coated coverslips, fixed using ice-cold methanol for 15 min, permeabilized by three 5-min washes with 0.6% Triton X-100 in phosphate-buffered saline (pH 7.4) followed by three 5-min washes with blocking solution (1% bovine serum albumin, 4% goat serum, and 0.3% Triton X-100 in phosphate-buffered saline, pH 7.4). The cells were incubated overnight at 4 °C with the sequence-specific antibodies for SERCA2a (1:500) and SERCA2b (1:500). In addition, paired samples of cells were incubated overnight at 4 °C with affinity-purified rabbit anti-RyR1 (1:500; raised against the peptide residues 4476–4486 (33)), anti-RyR2 (1:500; raised against the peptide residues 1344–1365 (34)), and anti-RyR3 (1:500; raised against the peptide residues 4236–4336 (35)). The coverslips were washed four times with blocking solution and incubated with goat anti-

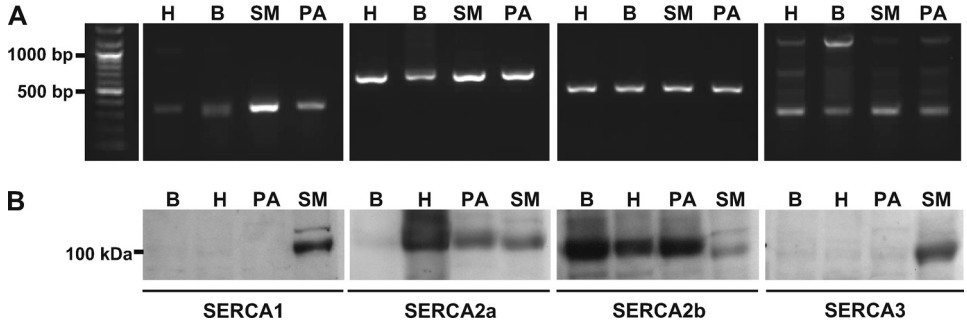

FIGURE 1. **SERCA2a and SERCA2b, but not SERCA1 or SERCA3, are functionally expressed in rat pulmonary arterial smooth muscle.** *A*, RT-PCR fragments of SERCA1, SERCA2a, SERCA2b, and SERCA3 amplified from total mRNA extracted from second and third order branches of the pulmonary arterial tree (*PA*), skeletal muscle (*SM*), heart (*H*), and brain (*B*) mRNAs. The predicted sizes of the PCR products were 340 bp for SERCA1, 694 bp for SERCA2a, 501 bp for SERCA2b, and 264 bp for SERCA3. *B*, Western blots for SERCA1, SERCA2a, SERCA2b, and SERCA3 in lysates of: smooth muscle from second order branches of the pulmonary arterial tree (*PA*), skeletal muscle (*SM*), heart (*H*), and brain (*B*). Each blot was also probed with an antibody selective for actin to ensure equal protein loading (not shown).

rabbit Texas Red-conjugated secondary antibody (1:200; excitation, 596 nm; emission, 620 nm). Then the coverslips were washed five times with phosphate-buffered saline and attached to slides by anti-fade mountant (2.4 g of Mowiol 4–88, 6 g of glycerol, 2 ml of 0.2 M Tris-HCl, pH 8.5, 2.5% 1,4-diazabicyclo(2.2.2.)octane) with 4′,6′-diamino-2-phenylindole (DAPI, 1 μg/ml; excitation, 358 nm; emission, 461 nm). For controls, the primary antibody was omitted. The images were acquired using a Deltavision imaging system (Applied Precision) consisting of an Olympus IX70 inverted microscope with an Olympus PlanApo 60×, 1.40 n.a. oil immersion objective and a Photometric CH300 charge-coupled device camera. Z section (0.2 μm) stacks were taken through cells. The images were deconvolved using Softworx acquisition and analysis software (Applied Precision) as described previously (18).

Analysis of Fluorescent Labeling—Three-dimensionally rendered images of pulmonary arterial smooth muscle cells were obtained using Volocity software (PerkinElmer Life Sciences) and subdivided into three defined volumes that excluded the DAPI-labeled nucleus, namely the perinuclear (the area of the cell located within 1.5 μm of the DAPI-labeled nucleus), the subplasmalemmal (the area of the cell located within 1.5 μm of the plasma membrane), and the extraperinuclear regions (the remaining volume of the cell). The volumes occupied by these three defined regions were measured, and then the density of fluorescent labeling in that region was determined by dividing the volume of protein labeling (*e.g.* for SERCA2a) within a given region by the volume of that region as described in detail previously (18). Thus, data are presented as the means ± S.E. of the volume of labeling per μm^3 of a given region ($\mu m^3/\mu m^3$).

Ca^{2+} Imaging—Pulmonary arterial smooth muscle cells (PASMCs) were incubated for 30 min with 5 μM Fura-2-AM in Ca^{2+}-free physiological salt solution in an experimental chamber on a Leica DMIRBE inverted microscope and then superfused with Fura-2-free physiological salt solution for at least 30 min prior to experimentation. Cytoplasmic Ca^{2+} concentration was reported by Fura-2 fluorescence ratio (F_{340}/F_{380} excitation; emission, 510 nm). Emitted fluorescence was recorded at 22 °C with a sampling frequency of 0.5 Hz using a Hamamatsu 4880 CCD camera via a Zeiss Fluar 40×, 1.3 n.a. oil immersion lens, and Leica DMIRBE microscope. Background subtraction was performed on-line. Analysis was via Openlab imaging software (Improvision).

Data Presentation and Statistical Analysis—The data are presented as the means ± S.E. Comparisons between the groups were carried out in MINITAB 14 using analysis of variance followed by a Tukey post-hoc test. Probability values less than 0.05 were considered to be statistically significant.

Drugs and Chemicals—All of the compounds were from Sigma-Aldrich except horseradish peroxidase-conjugated secondary antibodies (Vector Laboratories) and fluorescently tagged secondary antibodies (Jackson Immunoresearch).

RESULTS

Identification of SERCA Expressed in Pulmonary Arterial Smooth Muscle—RT-PCR products amplified from mRNA that was extracted from second and third order branches of the rat pulmonary arterial tree (without endothelium) identified transcripts for all SERCA subtypes after 40 cycles. These were consistent with the predicted sizes for SERCA1, SERCA2a, SERCA2b, and SERCA3 and matched the positive controls generated from mRNA extracted from rat brain, heart, and skeletal muscle (Fig. 1*A*). However, it is clear that the level of expression of SERCA2a and SERCA2b was higher than that observed with respect to the other subtypes.

The protein expression of SERCA isoforms was determined by Western blot. Specific antibodies against SERCA1, SERCA2a, SERCA2b, and SERCA3, respectively, detected appropriate bands of protein with a molecular mass of ~100 kDa in the lysate of control tissues, namely those for SERCA1, SERCA2a, and SERCA3 in skeletal muscle, SERCA2a and SERCA2b in heart, and SERCA2b in brain (Fig. 1*B*). However, Fig. 1*B* clearly shows that protein bands for SERCA2a and SERCA2b, but not for SERCA1 or SERCA3, were detected in paired samples from pulmonary arterial smooth muscle lysates.

SERCA2a and SERCA2b Are Differentially Distributed in Acutely Isolated Pulmonary Arterial Smooth Muscle Cells—Using sequence-specific antibodies against SERCA2a and SERCA2b, we confirmed the functional expression of SERCA2a and SERCA2b by immunocytochemistry and analyzed their respective spatial distributions by deconvolution microscopy. Strikingly, visual inspection of deconvolved images revealed discrete targeting of SERCA2a and SERCA2b to different regions of pulmonary arterial smooth muscle cells. Fig. 2*A* shows labeling for SERCA2a in an exemplar cell, which was almost entirely restricted to the perinuclear region. The dimensions of the cell are shown by a bright field image (*panel a*), adjacent images of a deconvolved Z-section through the cell

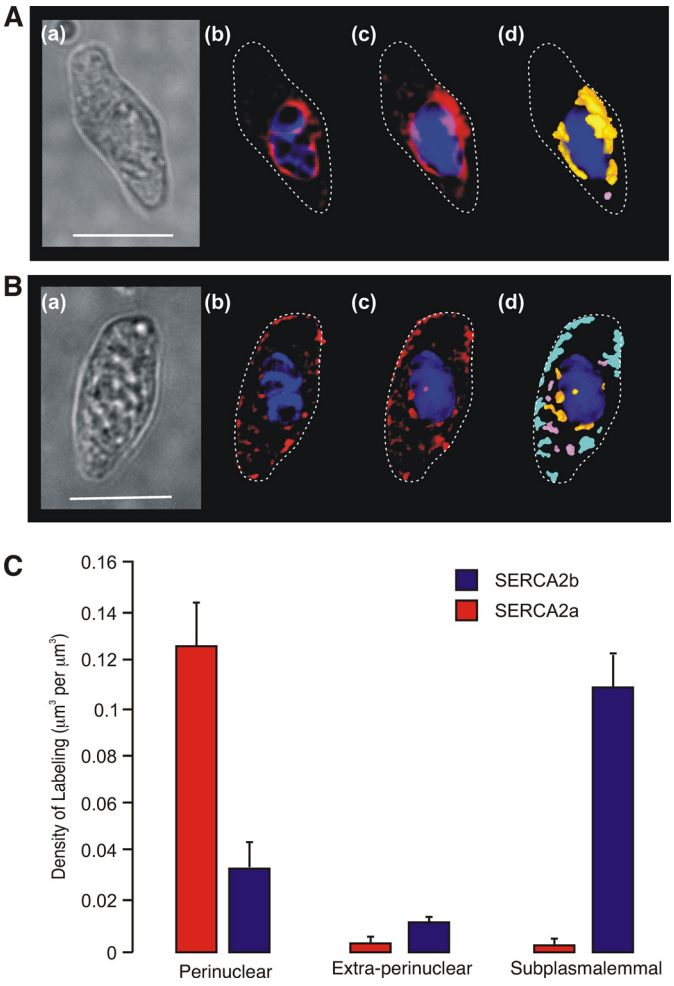

FIGURE 2. **SERCA2a and SERCA2b are differentially distributed within isolated pulmonary arterial smooth muscle cells.** *A* and *B*, images show the distribution of labeling for SERCA2a (*A*) and SERCA2b (*B*). *Panel a*, transmitted light image of PASMC. *Scale bar*, 10 μm. *Panel b*, deconvolved Z-section taken through the cell with labeling for the given SERCA subtype (*red*) in relation to the nucleus (*blue*) and the plasma membrane (*dotted line*). *Panel c*, three-dimensional reconstruction of a series of Z-sections (Z step 0.2 μm) obtained through the cell fluorescently labeled as in *panel b*. *Panel d*, three-dimensional representation showing the distribution by color of individual volumes of labeling for the given SERCA subtype in the perinuclear (*orange*), extraperinuclear (*pink*), and subplasmalemmal (*light blue*) regions. *C*, bar chart shows the density of labeling (μm^3 of labeling per μm^3; mean ± S.E.) for SERCA2a and SERCA2b within the three designated regions of isolated PASMCs.

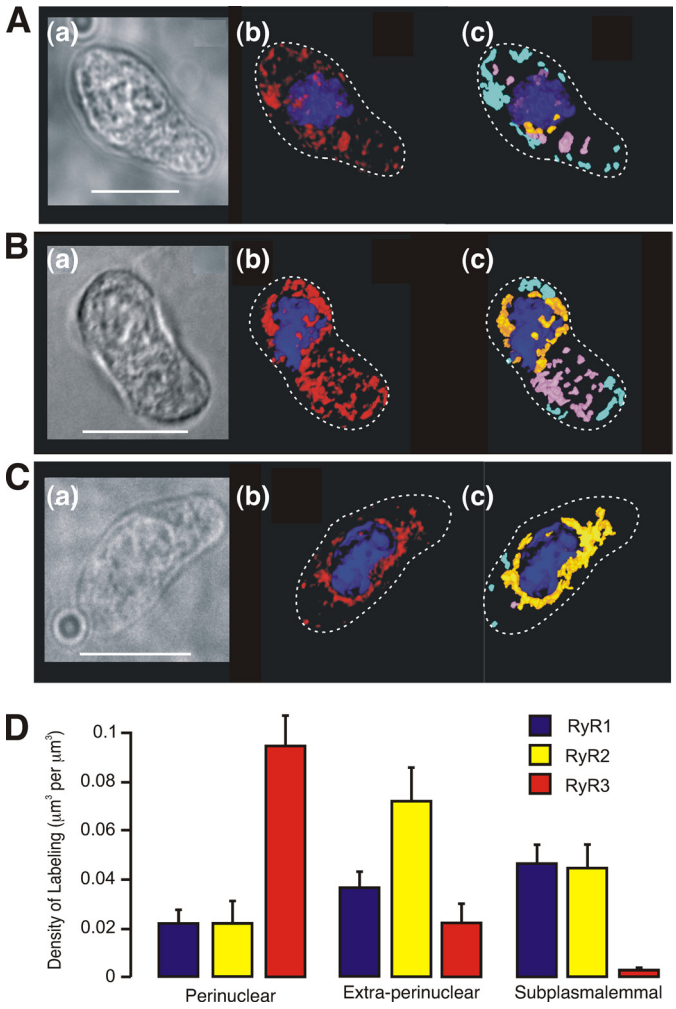

FIGURE 3. **RyR1, RyR2, and RyR3 are differentially distributed within isolated pulmonary arterial smooth muscle cells.** *A–C*, images show the distribution of labeling for RyR1 (*A*), RyR2 (*B*), and RyR3 (*C*). *Panel a*, transmitted light image of PASMC. *Scale bar*, 10 μm. *Panel b*, three-dimensional reconstruction of a series of Z-sections (Z step 0.2 μm) obtained through the cell fluorescently labeled in relation to the nucleus (*blue*) and the plasma membrane (*dotted line*). *Panel c*, three-dimensional representation showing the distribution by color of individual volumes of labeling for the given RyR subtype in the perinuclear (*orange*), extraperinuclear (*pink*), and subplasmalemmal (*light blue*) regions. *D*, bar chart shows the density of labeling (μm^3 of labeling per μm^3; means ± S.E.) for each of the RyR subtypes within the three designated regions of isolated PASMCs.

with the distribution of SERCA2a labeling in *red* relative to the DAPI-labeled nucleus in *blue* (*panel b*), and a three-dimensional reconstruction of a Z-stack of images showing the distribution of SERCA2a labeling (*panel c*) as in *panel b*. Fig. 2*A* (*panel d*) shows the three-dimensional reconstruction again, but this time with the distribution of labeling depicted by color across three defined volumes of the cell, namely the perinuclear region (*orange*; within 1.5 μm of, but excluding, the DAPI-labeled nucleus), the extraperinuclear region (*pink*), and the subplasmalemmal region (*light blue*; within 1.5 μm of the plasma membrane). Analysis of the distribution by density of SERCA2a labeling confirmed that it was almost entirely restricted to the perinuclear region of the cell, with the density of labeling in this region measuring 0.125 ± 0.019 $\mu m^3/\mu m^3$ ($p \leq 0.05$ when compared with SERCA2b, see below) compared with 0.003 ± 0.001 $\mu m^3/\mu m^3$ in the extraperinuclear region and 0.003 ± 0.002 $\mu m^3/\mu m^3$ in the subplasmalemmal region ($p \leq 0.01$ when compared with the perinuclear region; Fig. 3*C*). In marked contrast, SERCA2b appeared to be primarily located in close proximity to the plasma membrane. This is evident in Fig. 2*B*, which shows an exemplar cell as before, with a bright field image of the cell (*panel a*), a single deconvolved Z-section taken through the cell with the distribution of SERCA2b labeling again in *red* relative to the DAPI-labeled nucleus in *blue* (*panel b*), and a three-dimensional reconstruction of the associated Z-stack of images showing the distribution of labeling for SERCA2b (*panel c*) as in *panel b*. The discrete distribution of SERCA2b labeling in the three-dimensional image is clearer, however, when depicted by color (*panel d*) across the perinuclear region (*orange*; within 1.5 μm of, but excluding, the DAPI-labeled nucleus), the extraperinuclear region (*pink*), and the subplasmalemmal region (*light blue*; within 1.5 μm of the plasma membrane). The sub-

plasmalemmal targeting of SERCA2b was confirmed by analysis of the density of labeling, which measured 0.106 ± 0.016 $\mu m^3/\mu m^3$ ($p \leq 0.01$ when compared with SERCA2a) in the subplasmalemmal region compared with 0.010 ± 0.003 $\mu m^3/\mu m^3$ in the extraperinuclear region and 0.033 ± 0.011 $\mu m^3/\mu m^3$ in the perinuclear region (Fig. 2*C*; $p \leq 0.05$ when compared with the subplasmalemmal region). These findings suggest that SERCA2b serves an SR compartment proximal to the plasma membrane of pulmonary arterial smooth muscle cells, whereas SERCA2a serves a discrete SR compartment located centrally within these cells.

RyR1, RyR2, and RyR3 Are Differentially Distributed in Acutely Isolated Pulmonary Arterial Smooth Muscle Cells—Previous studies on RT-PCR products amplified from mRNA derived from rat pulmonary arterial smooth muscle have identified transcripts for all three RyR subtypes (17). Moreover, protein expression of each subtype has been confirmed in pulmonary arterial smooth muscle by Western blot and immunocytochemistry (17, 18) using affinity-purified sequence-specific antibodies that have been shown to be highly selective for RyR1 (33), RyR2 (34), and RyR3 (35) across a range of tissues in which they are expressed. Of greatest significance to the present study, however, is our previous finding that RyR3 may be preferentially targeted to regions of the SR that form junctional complexes with lysosomes to comprise a trigger zone for Ca^{2+} signaling by nicotinic acid adenine dinucleotide phosphate (18), with RyR1 and RyR2 preferentially targeted to regions of the SR that sit outside of the lysosome-SR junctions. Using the same affinity-purified antibodies, we therefore compared the distribution of each RyR subtype in cells from samples paired with those labeled for SERCA2a and SERCA2b, to determine whether or not SERCA2a and SERCA2b, respectively, clustered in regions of the cell occupied by different RyR subtypes to constitute functionally segregated SR compartments; the antibodies against the SERCA and RyR subtypes were all raised in rabbits and therefore precluded double labeling. The spatial distribution of each RyR subtype was analyzed as for SERCA (see above) and revealed discrete targeting of RyR1, RyR2, and RyR3. Fig. 3*A* shows labeling for RyR1 in an exemplar cell paired with those shown for SERCA2a and SERCA2b, with the dimensions of the cell provided by a typical bright field image (*panel a*), with adjacent images of a three-dimensional reconstruction of a Z-stack of images with the distribution of RyR1 labeling in *red* relative to the DAPI-labeled nucleus in *blue* (*panel b*), and the three-dimensional reconstruction again (*panel c*), but this time with the distribution of labeling depicted by color across the three different volumes within the cell, namely the perinuclear region (*orange*; within 1.5 μm of, but excluding, the DAPI-labeled nucleus), the extraperinuclear region (*pink*), and the subplasmalemmal region (*light blue*; within 1.5 μm of the plasma membrane). Analysis of the distribution by density of RyR1 labeling identified a progressive, although nonsignificant, increase in the density of RyR1 labeling from 0.0211 ± 0.005 $\mu m^3/\mu m^3$ in the perinuclear region, to 0.036 ± 0.007 $\mu m^3/\mu m^3$ in the extraperinuclear region and then to 0.046 ± 0.008 $\mu m^3/\mu m^3$ in the subplasmalemmal region where the majority of SERCA2b labeling was targeted (Fig. 3*D*, $n = 15$). In cells labeled for RyR2 (Fig. 3*B*), the distribution of labeling by density was different. Labeling by density was lowest in the perinuclear region at 0.022 ± 0.01 $\mu m^3/\mu m^3$, markedly higher in the extraperinuclear region measuring 0.072 ± 0.01 $\mu m^3/\mu m^3$ and then declined to 0.045 ± 0.01 $\mu m^3/\mu m^3$ in the subplasmalemmal region. In fact, labeling for RyR2 in the extraperinuclear region was not only markedly higher than that observed in the other two regions but was also 2–3-fold greater by density than labeling for either RyR1 or RyR3 within this region (Fig. 3*D*, $n = 10$; $p \leq 0.05$). In marked contrast to either RyR1 or RyR2 but consistent with the distribution of SERCA2a, Fig. 3*C* shows that labeling for RyR3 was almost entirely restricted to the perinuclear region of pulmonary arterial smooth muscle cells. Labeling by density measured 0.1 ± 0.01 $\mu m^3/\mu m^3$ in the perinuclear region compared with 0.02 ± 0.01 $\mu m^3/\mu m^3$ ($p \leq 0.05$) in the extraperinuclear region and 0.003 ± 0.001 $\mu m^3/\mu m^3$ ($p \leq 0.01$) in the subplasmalemmal region (Fig. 3*D*, $n = 10$).

These findings suggest that SERCA2a and RyR3 comprise a functionally segregated region of the SR proximal to the nucleus within pulmonary arterial smooth muscle cells. By contrast, it would appear that SERCA2b together with RyR1 may comprise a second, segregated SR compartment proximal to the plasma membrane. Between each of these, there appears to be a further region of the SR in which RyR2 is the predominant RyR subtype but with no clearly designated SERCA. Therefore, the SR within this region may receive Ca^{2+} from SERCA2a and/or SERCA2b because of the continuous nature of the SR Ca^{2+} store (12).

A Cyclopiazonic Acid-insensitive SR Ca^{2+} Store Underpins Calcium Signaling in Response to Endothelin-1—Previously we have shown that cyclopiazonic acid, a SERCA antagonist, inhibits vasodilation mediated by adenylyl cyclase-coupled β-adrenoreceptors (9), that is mediated, in part, by cAMP-dependent protein kinase- and cyclic ADP-ribose-dependent SR Ca^{2+} release via RyRs and consequent hyperpolarization that is driven by the subsequent recruitment of BK_{Ca} channels. We have also reported that a different SERCA antagonist, thapsigargin, blocks global Ca^{2+} waves triggered by the vasoconstrictor endothelin-1 (ET-1) (36). Importantly, in pulmonary arterial smooth muscle cells the ET-1-induced Ca^{2+} transient is mediated by an increase in nicotinic acid adenine dinucleotide phosphate levels, which triggers Ca^{2+} bursts from lysosomes that are subsequently amplified by Ca^{2+}-induced Ca^{2+} release from the SR via RyRs but not via IP_3 receptors (36, 37), and this has since been confirmed to be the case in coronary arterial smooth muscle cells (38). Given that previous studies on arterial smooth muscle cells had demonstrated the capacity of cyclopiazonic acid to deplete one of two releasable pools of Ca^{2+} within the SR (5), we therefore sought to determine whether or not cyclopiazonic acid and thapsigargin were equally effective at blocking global Ca^{2+} waves triggered by ET-1. Consistent with the proposal that different SERCA may serve functionally discrete SR compartments in pulmonary arterial smooth muscle, we observed quite different effects of these two different SERCA inhibitors. Fig. 4*A* shows a Ca^{2+} transient induced by ET-1 (100 nM) in an isolated pulmonary arterial smooth muscle cell, as indicated by an increase in the Fura-2 fluorescence ratio (F_{340}/F_{380}) from 0.49 ± 0.02 to 1.83 ±

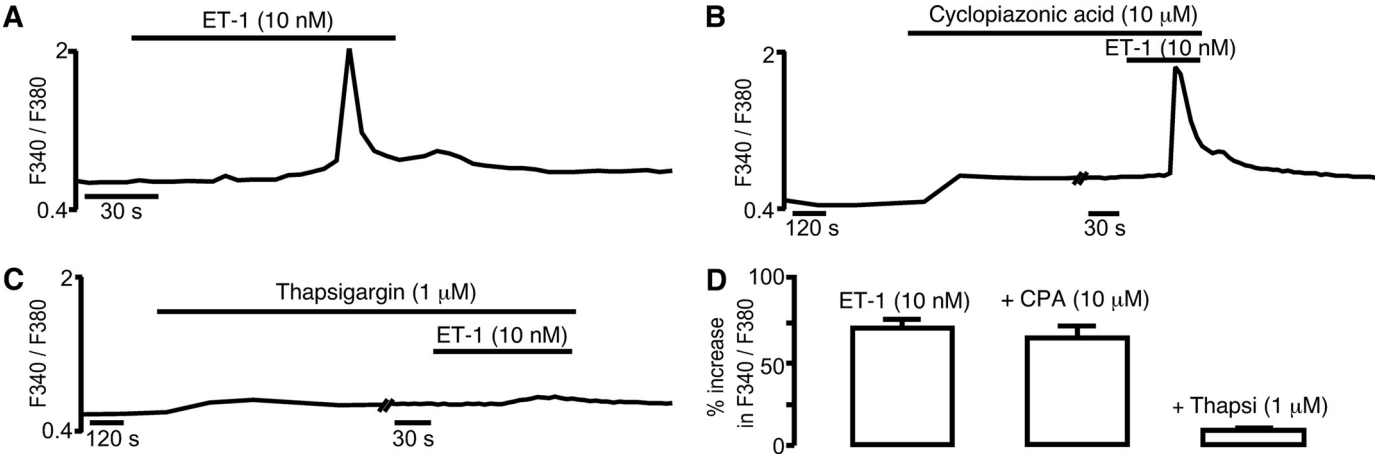

FIGURE 4. **A cyclopiazonic acid-insensitive sarcoplasmic reticulum Ca^{2+} store underpins Ca^{2+} signaling in response to ET-1 in pulmonary arterial smooth muscle cells.** *A–C*, the effect on the Fura-2 fluorescence ratio (F_{340}/F_{380}) in the absence (*A*) and presence of cyclopiazonic acid (*B*) and thapsigargin (*C*). *D*, bar chart shows the means ± S.E. for the percentage change in Fura-2 fluorescence ratio induced by ET-1 in the absence and presence of cyclopiazonic acid (*CPA*) and thapsigargin (*Thapsi*), respectively.

0.03 ($n = 31$). This remained unaffected following (Fig. 4*B*) preincubation (20 min) with cyclopiazonic acid (10 μM), with the Fura-2 fluorescence ratio rising from 0.59 ± 0.03 to 1.79 ± 0.05 ($n = 31$). In marked contrast, Fig. 4*C* shows that the Ca^{2+} transient induced by ET-1 was virtually abolished following preincubation (20 min) with thapsigargin (1 μM), the Fura-2 fluorescence ratio increasing from 0.52 ± 0.02 to 0.56 ± 0.03 ($n = 15$, $p \leq 0.01$). This fact is emphasized by the bar chart shown in Fig. 4*D*, which compares the means ± S.E. for the percentage increase in the Fura-2 fluorescence ratio at the peak of the Ca^{2+} transient induced by ET-1 under each condition. Thus, ET-1 triggers Ca^{2+} release from a cyclopiazonic acid-insensitive store in pulmonary arterial smooth muscle, whereas vasodilation by β-adrenoreceptor activation is mediated by Ca^{2+} release from a cyclopiazonic acid-sensitive SR store (9). In each case Ca^{2+} release has been shown to occur via RyRs, but with respect to vasodilation by β-adrenoreceptor activation, it is clear that the RyRs activated must sit proximal to the plasma membrane, because the released Ca^{2+} promotes vasodilation by opening BK_{Ca} channels (9). Therefore, these findings are entirely consistent with the presence of two functionally segregated SR Ca^{2+} stores being fed by two different SERCA subtypes, from which Ca^{2+} may be released via different populations of RyRs to elicit vasoconstriction and/or vasodilation. Given that SERCA2b and RyR1, but not SERCA2a or RyR3, sit proximal to the plasma membrane, it seems likely that SERCA2b supplies Ca^{2+} to a peripheral SR store that may be released via RyR1 to promote vasodilation in response to β-adrenoreceptor activation. By contrast SERCA2a and RyR3, likely coupled by Ca^{2+}-induced Ca^{2+} release to RyR2 in the perinuclear/extraperinuclear region (18), comprise the SR compartment responsible for initiation of propagating global Ca^{2+} waves and vasoconstriction. Moreover, these data suggest that SERCA2b exhibits a greater sensitivity to block by cyclopiazonic acid than does SERCA2a, at least under the conditions of our experiments.

DISCUSSION

In agreement with previous studies on vascular smooth muscle (32), our findings suggest that SERCA2a and SERCA2b are functionally expressed in pulmonary arterial smooth muscle. Strikingly, the vast majority of SERCA2b labeling (~72%) lay within the subplasmalemmal region (within 1.5 μm of the plasma membrane). In marked contrast, SERCA2a labeling was almost entirely (~90%) restricted to the perinuclear region of pulmonary arterial smooth muscle cells (within 1.5 μm of the perimeter of the nucleus). Consistent with the distribution of SERCA2a, RyR3 was almost entirely restricted to the perinuclear region (~70%). By contrast, RyR1 labeling was maximal in the subplasmalemmal region. These findings suggest that SERCA2a and RyR3 comprise a functionally segregated region of the SR proximal to the nucleus, whereas SERCA2b and RyR1 comprise a second, functionally segregated SR compartment proximal to the plasma membrane. Between these two regions, *i.e.* within the extraperinuclear volume, labeling for RyR2 was predominant, but with no clearly designated SERCA. The SR within this region may therefore receive Ca^{2+} from SERCA2a and/or SERCA2b because of the continuous nature of the SR Ca^{2+} store (12). This would be consistent with the view that RyR2 serves to carry, by Ca^{2+}-induced Ca^{2+} release, a propagating Ca^{2+} wave away from lysosome-SR junctions that sit within the perinuclear region, which cannot be achieved by RyR3 because it is restricted to the perinuclear region of the cell (18).

That there may be discrete SR compartments is supported by previous studies on arterial smooth muscle, the pulmonary vasculature included, and airway smooth muscle (4–7, 9, 11). In this respect, for each type of smooth muscle studied, the one key piece of evidence was that the SERCA pump antagonist cyclopiazonic acid exhibits the capacity to selectively deplete one of at least two functionally segregated SR compartments. Consistent with this view, we have previously shown that cyclopiazonic acid inhibits vasodilation of pulmonary arteries in response to β-adrenoreceptor activation by isoprenaline, which is mediated, in part, by Ca^{2+} release proximal to the plasma membrane via RyRs, consequent recruitment of plasmalemmal BK_{Ca} channels, smooth muscle cell hyperpolarization, and ultimately pulmonary artery dilation (9). In marked contrast to the block by cyclopiazonic acid of SR Ca^{2+} release in response to β-adrenoreceptor activation (9), we showed here

that global Ca^{2+} signals induced by ET-1, which are also carried by RyRs in pulmonary arterial smooth muscle cells, remained unaffected following preincubation with cyclopiazonic acid, but were abolished by preincubation of pulmonary arterial smooth muscle cells with thapsigargin, even though both drugs are SERCA antagonists. Thus, it seems likely that a cyclopiazonic acid-sensitive SERCA pump (SERCA2b) serves the SR compartment proximal to the plasma membrane, from which Ca^{2+} release via RyRs recruits plasmalemmal BK_{Ca} channels to elicit smooth muscle cell hyperpolarization and pulmonary artery dilation (9), whereas a SERCA pump that is relatively insensitive to cyclopiazonic acid (SERCA2a) serves a discrete SR compartment that underpins pulmonary artery constriction. Therefore, it is surprising to note that cell-free assays on recombinant SERCA2a and SERCA2b have shown that both cyclopiazonic acid and thapsigargin are effective inhibitors of both isoforms (39, 40). Thus, the preferential depletion of the peripheral SR store by cyclopiazonic acid is most likely due to its pharmacokinetics providing for "selective access" to SERCA2b over SERCA2a in a manner that may be determined by the local cytoplasmic environment (*e.g.* pH and ATP concentration) (41–43), the relative hydrophobicity of cyclopiazonic acid (Kp 3.1) and thapsigargin (Kp 4.9), and/or the fact that the affinity of cyclopiazonic acid for SERCA is 1,000 times lower than that of thapsigargin (44). However, in recombinant systems, it has been shown that SERCA2b can be selectively inhibited by monovalent cations such as Cs^{+} (45). Furthermore, cyclopiazonic acid and thapsigargin occupy different nonoverlapping binding sites in the ATPase (43), and site-directed mutagenesis of SERCA can selectively reduce the affinity of cyclopiazonic acid relative to thapsigargin (46). Thus, we cannot rule out the possibility that post-translational modifications could confer a pharmacology distinct from that exhibited by recombinant SERCA.

Given our findings, it may be important to note that SERCA2a and SERCA2b exhibit distinct kinetics. SERCA2b, which our data suggest serves a peripheral SR store that underpins Ca^{2+}-dependent vasodilation, has a higher affinity for Ca^{2+} but a lower V_{max} than SERCA2a (47–49), which our data suggest serves a central SR compartment that supports vasoconstriction. SERCA2b may therefore be dominant at rest and function to maintain resting levels of Ca^{2+} in the vicinity of the contractile apparatus. However, its low V_{max} may lead to saturation of this SERCA with Ca^{2+} upon release of Ca^{2+} from the central SR compartment in response to stimuli that elicit vasoconstriction. Thereby, SERCA2b would allow the Ca^{2+} concentration to rise in the vicinity of the contractile apparatus, until such time as vasodilation is promoted by adenylyl cyclase-coupled receptors that may: 1) increase the activity of SERCA2b by phosphorylation via cAMP-dependent protein kinase (50, 51) and facilitate the removal of Ca^{2+} from the greater cytoplasm and 2) trigger Ca^{2+} release from the peripheral SR store via RyRs in a manner mediated by cAMP-dependent protein kinase, leading to plasma membrane hyperpolarization and secondary facilitation of Ca^{2+} sequestration from the junctional space between the SR and the plasma membrane via the Na^{+}/Ca^{2+} exchanger (2, 52) and/or plasma membrane Ca^{2+}-ATPase (Fig. 5). This has a physiological precedent in that it

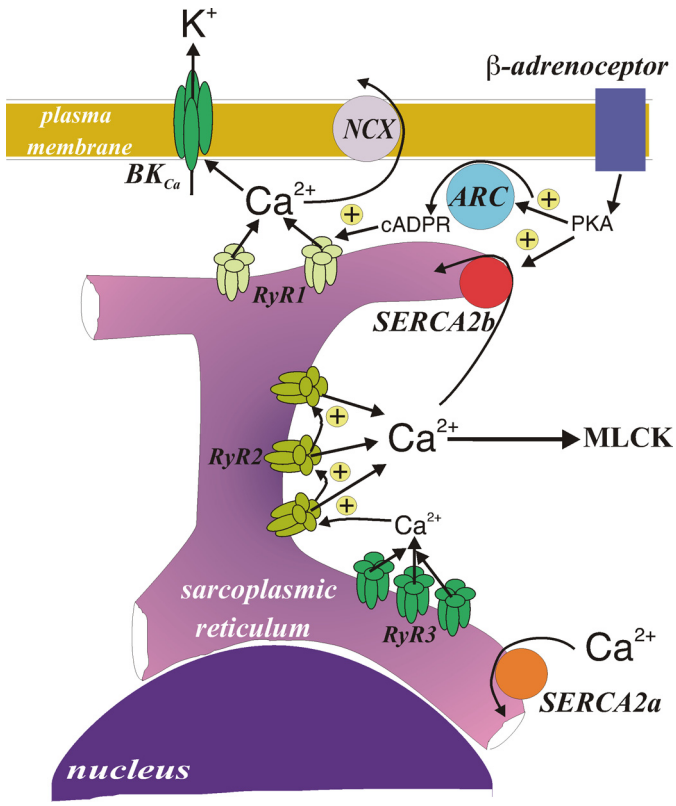

FIGURE 5. **Schematic representation of the spatial and functional compartmentalization of the sarcoplasmic reticulum in a pulmonary arterial smooth muscle cell.** *NCX*, sodium/calcium exchanger; *PKA*, cAMP-dependent protein kinase; *ARC*, ADP-ribosyl cyclase; *cADPR*, cyclic adenosine diphosphate-ribose; *MLCK*, myosin light chain kinase.

mirrors somewhat the roles of uptake 1 and uptake 2 at noradrenergic synapses, which are also dependent on the relative affinity and V_{max} of these two catecholamine transporters.

In summary, the present investigation provides evidence in support of the view that there may be two functionally segregated SR Ca^{2+} stores within pulmonary arterial smooth muscle cells, each served by a different SERCA pump. One may lie in close apposition to the plasma membrane, is likely served by SERCA2b, and likely releases Ca^{2+} via RyR1 to promote pulmonary artery dilation (9). The other appears to be located centrally, is served by SERCA2a, and releases Ca^{2+} via RyR3, which may in turn recruit RyR2 by Ca^{2+}-induced Ca^{2+} release to elicit a propagating global Ca^{2+} wave (18) and consequent pulmonary artery constriction (10, 11, 18).

REFERENCES

1. Nazer, M. A., and van Breemen, C. (1998) *Cell Calcium* **24,** 275–283
2. van Breemen, C., Chen, Q., and Laher, I. (1995) *Trends Pharmacol. Sci.* **16,** 98–105
3. Iino, M., Kobayashi, T., and Endo, M. (1988) *Biochem. Biophys. Res. Commun.* **152,** 417–422
4. Janiak, R., Wilson, S. M., Montague, S., and Hume, J. R. (2001) *Am. J. Physiol. Cell Physiol.* **280,** C22–C33
5. Golovina, V. A., and Blaustein, M. P. (1997) *Science* **275,** 1643–1648
6. Tribe, R. M., Borin, M. L., and Blaustein, M. P. (1994) *Proc. Natl. Acad. Sci. U.S.A.* **91,** 5908–5912
7. Ethier, M. F., Yamaguchi, H., and Madison, J. M. (2001) *Am. J. Physiol. Lung Cell Mol Physiol* **281,** L126–L133
8. Yamaguchi, H., Kajita, J., and Madison, J. M. (1995) *Am. J. Physiol.* **268,** C771–C779

9. Boittin, F. X., Dipp, M., Kinnear, N. P., Galione, A., and Evans, A. M. (2003) *J. Biol. Chem.* **278,** 9602–9608
10. Dipp, M., Nye, P. C., and Evans, A. M. (2001) *Am. J. Physiol. Lung Cell Mol. Physiol.* **281,** L318–L325
11. Dipp, M., and Evans, A. M. (2001) *Circ. Res.* **89,** 77–83
12. McCarron, J. G., and Olson, M. L. (2008) *J. Biol. Chem.* **283,** 7206–7218
13. Evans, A. M., Wyatt, C. N., Kinnear, N. P., Clark, J. H., and Blanco, E. A. (2005) *Pharmacol. Ther.* **107,** 286–313
14. Fleischer, S. (2008) *Biochem. Biophys. Res. Commun.* **369,** 195–207
15. Herrmann-Frank, A., Darling, E., and Meissner, G. (1991) *Pflugers Arch.* **418,** 353–359
16. Neylon, C. B., Richards, S. M., Larsen, M. A., Agrotis, A., and Bobik, A. (1995) *Biochem. Biophys. Res. Commun.* **215,** 814–821
17. Yang, X. R., Lin, M. J., Yip, K. P., Jeyakumar, L. H., Fleischer, S., Leung, G. P., and Sham, J. S. (2005) *Am. J. Physiol. Lung Cell Mol. Physiol.* **289,** L338–L348
18. Kinnear, N. P., Wyatt, C. N., Clark, J. H., Calcraft, P. J., Fleischer, S., Jeyakumar, L. H., Nixon, G. F., and Evans, A. M. (2008) *Cell Calcium* **44,** 190–201
19. Brandl, C. J., Green, N. M., Korczak, B., and MacLennan, D. H. (1986) *Cell* **44,** 597–607
20. Lytton, J., and MacLennan, D. H. (1988) *J. Biol. Chem.* **263,** 15024–15031
21. Gunteski-Hamblin, A. M., Greeb, J., and Shull, G. E. (1988) *J. Biol. Chem.* **263,** 15032–15040
22. Burk, S. E., Lytton, J., MacLennan, D. H., and Shull, G. E. (1989) *J. Biol. Chem.* **264,** 18561–18568
23. Brandl, C. J., deLeon, S., Martin, D. R., and MacLennan, D. H. (1987) *J. Biol. Chem.* **262,** 3768–3774
24. Korczak, B., Zarain-Herzberg, A., Brandl, C. J., Ingles, C. J., Green, N. M., and MacLennan, D. H. (1988) *J. Biol. Chem.* **263,** 4813–4819
25. Bobe, R., Bredoux, R., Wuytack, F., Quarck, R., Kovàcs, T., Papp, B., Corvazier, E., Magnier, C., and Enouf, J. (1994) *J. Biol. Chem.* **269,** 1417–1424
26. Wuytack, F., Papp, B., Verboomen, H., Raeymaekers, L., Dode, L., Bobe, R., Enouf, J., Bokkala, S., Authi, K. S., and Casteels, R. (1994) *J. Biol. Chem.* **269,** 1410–1416
27. Poch, E., Leach, S., Snape, S., Cacic, T., MacLennan, D. H., and Lytton, J. (1998) *Am. J. Physiol.* **275,** C1449–C1458
28. Martin, V., Bredoux, R., Corvazier, E., Van Gorp, R., Kovacs, T., Gelebart, P., and Enouf, J. (2002) *J. Biol. Chem.* **277,** 24442–24452
29. Bobe, R., Bredoux, R., Corvazier, E., Andersen, J. P., Clausen, J. D., Dode, L., Kovács, T., and Enouf, J. (2004) *J. Biol. Chem.* **279,** 24297–24306
30. Wuytack, F., Eggermont, J. A., Raeymaekers, L., Plessers, L., and Casteels, R. (1989) *Biochem. J.* **264,** 765–769
31. Mahmmoud, Y. A., Cramb, G., Maunsbach, A. B., Cutler, C. P., Meischke, L., and Cornelius, F. (2003) *J. Biol. Chem.* **278,** 37427–37438
32. Eggermont, J. A., Wuytack, F., Verbist, J., and Casteels, R. (1990) *Biochem. J.* **271,** 649–653
33. Jeyakumar, L. H., Gleaves, L. A., Ridley, B. D., Chang, P., Atkinson, J., Barnett, J. V., and Fleischer, S. (2002) *J. Muscle Res. Cell Motil.* **23,** 285–292
34. Jeyakumar, L. H., Ballester, L., Cheng, D. S., McIntyre, J. O., Chang, P., Olivey, H. E., Rollins-Smith, L., Barnett, J. V., Murray, K., Xin, H. B., and Fleischer, S. (2001) *Biochem. Biophys. Res. Commun.* **281,** 979–986
35. Jeyakumar, L. H., Copello, J. A., O'Malley, A. M., Wu, G. M., Grassucci, R., Wagenknecht, T., and Fleischer, S. (1998) *J. Biol. Chem.* **273,** 16011–16020
36. Kinnear, N. P., Boittin, F. X., Thomas, J. M., Galione, A., and Evans, A. M. (2004) *J. Biol. Chem.* **279,** 54319–54326
37. Boittin, F. X., Galione, A., and Evans, A. M. (2002) *Circ. Res.* **91,** 1168–1175
38. Zhang, F., Zhang, G., Zhang, A. Y., Koeberl, M. J., Wallander, E., and Li, P. L. (2006) *Am. J. Physiol. Heart Circ. Physiol.* **291,** H274–H282
39. Campbell, A. M., Kessler, P. D., Sagara, Y., Inesi, G., and Fambrough, D. M. (1991) *J. Biol. Chem.* **266,** 16050–16055
40. Verboomen, H., Wuytack, F., De Smedt, H., Himpens, B., and Casteels, R. (1992) *Biochem. J.* **286,** 591–595
41. Inesi, G., Lewis, D., Toyoshima, C., Hirata, A., and de Meis, L. (2008) *J. Biol. Chem.* **283,** 1189–1196
42. Hauser, K., and Barth, A. (2007) *Biophys. J.* **93,** 3259–3270
43. Jensen, A. M., Sørensen, T. L., Olesen, C., Møller, J. V., and Nissen, P. (2006) *EMBO J.* **25,** 2305–2314
44. Moncoq, K., Trieber, C. A., and Young, H. S. (2007) *J. Biol. Chem.* **282,** 9748–9757
45. Kargacin, G. J., Aschar-Sobbi, R., and Kargacin, M. E. (2005) *Pflugers Arch.* **449,** 356–363
46. Ma, H., Zhong, L., Inesi, G., Fortea, I., Soler, F., and Fernandez-Belda, F. (1999) *Biochemistry* **38,** 15522–15527
47. Odermatt, A., Kurzydlowski, K., and MacLennan, D. H. (1996) *J. Biol. Chem.* **271,** 14206–14213
48. Dode, L., Andersen, J. P., Leslie, N., Dhitavat, J., Vilsen, B., and Hovnanian, A. (2003) *J. Biol. Chem.* **278,** 47877–47889
49. Verboomen, H., Wuytack, F., Van den Bosch, L., Mertens, L., and Casteels, R. (1994) *Biochem. J.* **303,** 979–984
50. Lindemann, J. P., Jones, L. R., Hathaway, D. R., Henry, B. G., and Watanabe, A. M. (1983) *J. Biol. Chem.* **258,** 464–471
51. Raeymaekers, L., Eggermont, J. A., Wuytack, F., and Casteels, R. (1990) *Cell Calcium* **11,** 261–268
52. Nazer, M. A., and Van Breemen, C. (1998) *Am. J. Physiol.* **274,** H123–H131